Multisensory integration enhances audiovisual responses in the Mauthner cell

Santiago Otero-Coronel[1], Thomas Preuss[2] and Violeta Medan[1,3]*

Abbreviated title: Multisensory integration in the Mauthner cell

1. Instituto de Fisiología y Biología Molecular y Celular, Consejo Nacional de Investigaciones Científicas y Tecnológicas, Buenos Aires, Argentina (1428).
2. Dept. Psychology, Hunter College, City University of New York, New York, NY, USA (10065).
3. Dept. Fisiología y Biología Molecular y Celular, Facultad de Ciencias Exactas y Naturales, Universidad de Buenos Aires, Buenos Aires, Argentina (1428).

*Corresponding author, e-mail: violetamedan@fbmc.fcen.uba.ar.

Conflict of interest statement: The authors declare no competing financial interests.

ABSTRACT

Multisensory integration combines information from multiple sensory modalities to create a coherent perception of the world. In contexts where sensory information is limited or equivocal, it also allows animals to integrate individually ambiguous stimuli into a clearer or more accurate percept and, thus, react with a more adaptive behavioral response. Although responses to multisensory stimuli have been described at the neuronal and behavioral levels, a causal or direct link between these two is still missing. In this study, we studied the integration of audiovisual inputs in the Mauthner cell, a command neuron necessary and sufficient to trigger a stereotypical escape response in fish. We performed intracellular recordings in adult goldfish while presenting a diverse range of stimuli to determine which stimulus properties affect their integration. Our results show that stimulus modality, intensity, temporal structure, and interstimulus delay affect input summation. Mechanistically, we found that the distinct decay dynamics of feedforward inhibition triggered by auditory and visual stimuli can account for certain aspects of input integration. Altogether, this is a rare example of the characterization of multisensory integration in a cell with clear behavioral relevance, providing both phenomenological and mechanistic insights into how multisensory integration depends on stimulus properties.

INTRODUCTION

The ability to detect a potential threat and react with an escape behavior is critical for survival. In nature, however, many predators develop strategies such as camouflage or partial hiding to decrease their salience, and sensory stimuli tend to be noisy and ambiguous. Consequently, it is adaptive for animals to have ways to disambiguate the signals from the sensory inflow they receive, especially in contexts where available information is limited.

One strategy for reducing sensory uncertainty is multisensory integration (MSI), which is defined as the process of combining information coming from multiple sensory streams to form a new percept with reduced ambiguity (Stein and Stanford, 2008). MSI has been extensively documented in animals from nematodes to humans and in a broad range of behavioral contexts (Wallace et al., 1998; Metaxakis et al., 2018; Zhou et al., 2019; Gil-Guevara et al., 2022). In the context of escape behaviors, MSI of threat-like stimuli increases the escape probability and reduces the latency of the evoked response (Rowland et al., 2007; Martorell and Medan, 2022). In mammals, activation of different parts of the superior colliculus determines whether animals engage in exploratory or defensive behaviors (Dean et al., 1989; Wei et al., 2015). Importantly, the superior colliculus contains neurons that integrate multisensory stimuli due to synaptic convergence of afferents conveying information from different sensory modalities (Kadunce et al., 2001). These studies established that the effects of MSI are larger when weak or ambiguous stimuli are combined, thus showing an inverse effectiveness relationship with stimulus strength. The underlying hypothesis is that integration of sensory signals from different modalities form a more accurate world percept only if each unisensory signal carries some uncertainty or ambiguity.

In goldfish, audiovisual MSI increases the probability and reduces the latency of startle escape behaviors, with an inverse relationship between the MSI effectiveness and the stimulus salience (McIntyre and Preuss, 2019; Martorell and Medan, 2022). These startle escapes (C-starts) are triggered by a pair of reticulospinal neurons (Mauthner cells) that receive visual and auditory inputs through anatomically segregated pathways. Auditory inputs reach the M-cell lateral dendrite through a disynaptic (2 ms) pathway, while the visual inputs relay information in the optic tectum before reaching the M-cell ventral dendrite through a polysynaptic (20 ms) pathway (Zottoli et al., 1987; Pereda et al., 2004; Korn and Faber, 2005; Szabo et al., 2007). Interestingly, the auditory and visual M-cell dendrites show differences in their cable properties, which appear to be well suited to process inputs from abrupt (i.e. fast raise time) auditory pips and more gradually raising visual looms (Medan et al., 2017). However, it is unclear how auditory and visual signals are integrated at the level of the M-cell to generate a multisensory response.

The accessibility of M-cells for *in vivo* intracellular recordings provides an excellent opportunity to investigate the cellular mechanisms of multisensory integration. Moreover, the one-to-one relationship between a single M-cell action potential and the initiation of a C-start (Zottoli, 1977; Weiss et al., 2006; Zwaka et al., 2022) provides a clear link between behavior and the observed integration in the M-cell. As such, the goal of this study was to reveal the cellular mechanism that underlie the multimodal integration of M-cell initiated startle escapes we observed in the behavioral experiments (McIntyre and Preuss, 2019; Martorell and Medan, 2022). Specifically, we studied how visual and auditory presynaptic pathways and intrinsic membrane properties of the M-cell interact to produce MSI to ultimately enhance threat detection. To this end, we performed intracellular *in vivo* recordings from the M-cell soma using auditory and tectal stimuli with naturalistic dynamics (Preuss et al., 2006; Szabo et al., 2006; Medan et al., 2017). Our results show that the temporal dynamics and strength of stimuli, as well as sensory evoked feed-forward inhibition affect the magnitude of MSI. The results represent a rare characterization of MSI at a single-cell level in a neuron that is sufficient and necessary to trigger a distinct behavior.

METHODS

Animals

We used adult goldfish (*Carassius auratus*) of both sexes and 7–10 cm of standard body length. Fish were purchased from Billy Bland Fishery (Taylor, AR, USA), Hunting Creek Fisheries (Thurmont, MD, USA) or Daniel Corriarello Aquarium (Buenos Aires, Argentina) and allowed to acclimate for at least a week after transport. Fish were kept in rectangular Plexiglas holding tanks (30 x 60 x 30 cm^3; 54 l) in groups of up to 10 individuals. Tanks were supplied with filtered and dechlorinated water and maintained at 18 °C. Ambient light was set to a 12-h light/dark photoperiod. Animals were fed floating pellets (Sera, Germany) five times a week. All procedures and protocols were performed in accordance with the guidelines and regulations of the Institutional Animal Care and Use Committee of Hunter College, City University of New York and Facultad de Ciencias Exactas y Naturales, Universidad de Buenos Aires.

Auditory stimuli

Sound stimuli consisted in single-cycle sound pips (5-ms duration at 200 Hz) produced by a function generator (33210A Agilent Technologies Inc., Santa Clara, CA, USA) connected to a shielded subwoofer (SA-WN250 Sony Corp., Tokyo, Japan) located 30 cm to the right from the recording chamber. Sound stimuli were recorded with a microphone (XM8500, Behringer) positioned 10 cm over the head of the fish. Calibration recordings were performed with a hydrophone (SQ01, Sensor Technology, Ontario, Canada) positioned where the submerged fish was placed during experiments. Since we were interested in studying integration of subthreshold stimuli, we used sound intensities known to be subthreshold for evoking behavioral startle responses (Neumeister et al., 2008; Weiss et al., 2009; Martorell and Medan, 2022). For all experiments we used a sound intensity of 118 dB SPL (relative to 1 μPa in water), except for the experiments in Figure 4 where we used a sound intensity of 147 dB SPL (relative to 1 μPa in water). Post-hoc analysis of the M-cell responses in this study revealed that only 3 out of 60 M-cells (5%) fired at least once to an auditory stimulus.

Optic tectum stimulation

Tectal stimuli were administered to the mid-anterior rim of the left tectum using a bipolar electrode (#30202 FHC, Bowdoin, ME, USA) connected to an isolated stimulator (DS2A; Digitimer Ltd, Welwyn Garden City, UK). In most cases, stimulation [100 µs, 0.1-1mA] in this area was effective in driving subthreshold responses (< 4 mV) in the M-cell. To change the strength and dynamics of the tectal stimulation we either used a 60-Hz stimulation train of variable duration (1, 33, 66, 100, 200 ms) or a 100-ms train of variable frequency (1, 33, 100, 200 Hz). We deliberately used tectal stimuli that

evoked M-cell firing with a very low probability (6.7%, 4 out of 60 M-cells tested fired at least once to any of the tectal stimuli used).

Electrophysiology

M-cell intracellular responses to tectal and acoustic stimuli were studied *in vivo* using standard surgical and electrophysiological recording techniques (Preuss and Faber, 2003; Preuss et al., 2006; Medan et al., 2017). To initiate anesthesia, fish were immersed in 1 liter of ice water with 40 mg/l of the general anesthetic tricaine methanesulfonate (MS-222, Western Chemical, Ferndale, WA, USA), until the fish ceased to swim, lost equilibrium and were unresponsive to a pinch on the tail (typically 10–15 min). They were next treated with 20% benzocaine gel (Ultradent, South Jordan, UT, USA) at incision sites and pin-holding points 5 min prior to surgical procedures. Fish were stabilized in the recording chamber by two pins, one on each side of the head, and ventilated through the mouth with recirculating, aerated saline at 18°C (saline [g/l]: sodium chloride 7.25, potassium chloride 0.38, monosodium phosphate monobasic 0.39, magnesium sulfate 0.11, Hepes 4.77; calcium chloride 0.24; dextrose 1.01, pH 7.2). The recording chamber was mounted inside an opaque, thin-walled tank filled with saline that covered the fish up to eye level. The recirculating saline also included a maintenance concentration of the anesthetic MS-222 (20 g/l) that does not interfere with auditory processing (Palmer and Mensinger, 2004; Cordova and Braun, 2007). Next, the spinal cord was exposed with a small lateral incision at the caudal midbody. Bipolar stimulation electrodes were placed on the unopened spinal cord to transmit low-intensity (5–8 V) electrical pulses generated by an isolated stimulator (A 360, WPI, Sarasota, FL, USA). This allowed antidromic activation of the M-cell axons, as confirmed by a visible muscular contraction (twitch). Surgical procedures were performed before a muscle paralysis agent was injected, which allows monitoring the effectiveness of the anesthetic by watching for an increase of opercula movement frequency (largely reduced in deep anesthesia) and movements/twitches in response to the surgical procedures. Shortly before the recordings started, animals were injected I.M. with D-tubocurarine (1 μg g^{-1} b.w.; Abbott Laboratories, Abbott Park, IL, USA) and a small craniotomy exposed the medulla for electrophysiological recordings. Antidromic stimulation produces a negative potential in the M-cell axon cap (typically 15–20 mV), which unambiguously identifies the axon hillock and allows intracellular recordings from defined locations along the M-cell soma-dendritic membrane (Furshpan and Furukawa, 1962; Furukawa, 1966; Faber and Korn, 1989). Intracellular recordings were acquired using borosilicate glass electrodes (7–10 MΩ) filled with 5 M potassium acetate and an Axoclamp-2B amplifier (Axon Instruments, Foster City, CA, USA) in current-clamp setting. M-cell responses were acquired with a Digidata 1440A (Axon Instruments) at 25 kHz. Electrodes were advanced using

motorized micromanipulators (MP-285; Sutter Instruments, Novato, CA, USA) until reaching the axon cap (defined as a site with an extracellular M-cell AP field >10 mV). Next, the electrode was moved 50 μm lateral and 50 μm posterior to penetrate the somatic region. Only trials in which the resting membrane potential was between -90 and -70 mV were included in the analysis.

Statistical Analyses and Experimental Design

To perform statistical analysis, we used R (version 4.0.2, www.r-project.org) and RStudio (version 1.1.456, www. rstudio. com). A significance level of α = 0.05 was used throughout the study. Effects of explanatory variables over response variables were assessed using Linear Models followed by ANOVA or binomial GLMs in the case of binary variables. Paired T-tests were used to compare tectal or auditory responses recorded in left or right M-cells (see Fig. 1). Two tailed Wilcoxon Ranked Sum tests were used for single sample comparisons. Sample size is denoted by N when it refers to the number of goldfish, *n* when it refers to the number of trials (average of 5-10 presentations). In experiments where we recorded from both M-cells of the same animals, results were pooled. Boxplots show the median, 25 and 75th percentile, and lines indicate minimum and maximum values.

Postsynaptic responses to acoustic and tectal stimuli were recorded at the M-cell soma and averages of 5-10 responses were used in the statistical analysis. M-cell responses to trains of tectal stimulation consist of phasic postsynaptic potentials riding on top of a tonic depolarizing response (Figure 1A-C). We analyzed the contribution of the phasic and tonic components separately (Figure 1A´). To do this we considered a 12 ms window following the last tectal pulse (color-shaded areas in Figure 1A-C) and defined the tonic response amplitude as the difference between the membrane potential immediately before the arrival of the last pulse (blue bar on Figure 1A´) and resting membrane potential. The phasic response was defined as the difference between the peak voltage in response to the last train pulse and the depolarization reached immediately before the last tectal pulse (orange bar on Figure 1A´).

To characterize multisensory integration, we quantified responses calculating the mean evoked depolarization in a 12 ms window after sound onset (auditory only trials, A) or after the last tectal stimulus in tectal-only (tectal only trials, T) and multisensory (tectal + auditory trials, M) trials (Fig. 2), considering both phasic and tonic components. We also measured the peak amplitude of the response, which in all cases occurred in the same time window. As peak amplitude analysis resulted in the same qualitative results, only the mean area analysis is shown.

For quantification, the responses to M stimuli were normalized to the T and A components. In the field of multisensory integration, multisensory responses are typically normalized to the maximum

response of the unisensory stimulus (Meredith and Stein, 1983; Stanford and Stein, 2007; Stein and Stanford, 2008), which we call Multisensory-Maximum Unimodal index (MSI/Max):

$$MSI/Max = M \div max(T,\ A)$$

The value of this index determines the net effect of the integration, where M is the multisensory response and max(T, A) is the largest of the two unisensory components (all evaluated as the area in a 12-ms window as defined above). Therefore, a *MSI/Max* greater than 1 represents multisensory enhancement, *MSI/Max* lower than 1 represents multisensory inhibition, and *MSI/Max* not significantly different than 1 suggests absence of multisensory integration (Stein and Stanford, 2008). Additionally, to calculate the linearity of the multisensory integration performed by the M-cell, we calculated the ratio between the multisensory response and the sum of the unisensory responses, which we call Multisensory-Sum Unimodals index (MSI/Sum):

$$MSI/Sum = M \div (T + A)$$

The value of this index indicates the linearity of the integration, determined by the ratio of the multisensory response M and the sum of the unisensory components, T and A. MSI/Sum greater than 1 representing supralinear integration, MSI/Sum of 1 representing linear integration, and MSI/Sum lower than 1 representing sublinear integration (Stanford et al., 2005).

The M-cell is subject to feedforward inhibition which can be triggered by either auditory or tectal stimuli (Faber and Korn, 1982; Medan et al., 2017). Evoked FFI can be quantified as the amplitude reduction of an antidromically evoked “test” action potential (APtest) after presenting a single auditory pip or a brief tectal train as “conditioning” stimuli of similar strength. Both stimuli evoked comparable peak depolarizations in the M-cell (~5 mV). To test if FFI evoked by auditory or tectal stimuli differed, we evoked the APtest at specific times (2–80 ms) following a sensory stimulus and calculated shunting inhibition as %SI= 100 - APtest/APcontrol ×100, where AP control is the amplitude of the AP without a conditioning stimulus (Figure 3A).

One of the principles that guide multisensory integration is the spatial coherence of the different cues being integrated. If the perceived source localizations of two stimuli overlap, these stimuli are

more likely to be integrated. Conversely, if the two stimuli arrive from spatially disparate sources the chances of observing a multisensory integration will decrease (Meredith and Stein, 1996; Stein and Stanford, 2008). The geometrical configuration of the setup in our experiments determined that the loudspeaker used to produce acoustic stimuli was mounted to the right of the fish and electrical stimulation was applied to the left tectum (which normally receives visual signals from the right retina). Whenever possible, we performed recordings from both Mauthner cells. To rule out the possibility of a systematic difference on the responses of either M-cell due to the spatial source of the stimuli, we compared the responses to tectal or auditory stimuli in sequential recordings of the right and left M-cells of the same fish. Supplementary Figure 1 shows representative trace examples for tectal (100 ms 60 Hz tectal train, Fig. Supp. 1A) and auditory (5 ms 200 Hz auditory pip, Fig. Supp. 1B) stimulation from the left (upper traces) or right (lower traces) M-cell of the same fish. The complex post-synaptic potentials were highly stereotypical in successive presentations of a T or A stimuli within and across cells. Analysis from pairs of tectal (Fig. Supp. 1C, N=9) and auditory (Fig. Supp. 1D, N=11) M-cell responses showed no statistical differences between ipsi- and contralateral stimulation (paired T-test, T: $t(8)= 0.18$, $p=0.8573$, A: $t(10)= -0.76$, $p=0.4672$). This confirms previous results indicating that in goldfish, tectal stimulation produces responses with similar latency and amplitude in both M-cells (Zottoli et al., 1987; Canfield, 2006). We therefore pooled data acquired from left or right M-cells for all following analysis.

RESULTS

MAUTHNER CELL RESPONSES ARE SENSITIVE TO THE DYNAMICS OF TECTAL STIMULI

Multisensory integration is known to be dependent on the saliency of the unimodal components (Stanford et al., 2005; Martorell and Medan, 2022). To create a stimulus set of variable strength and temporal dynamics, we recorded M-cell responses to different electrical trains delivered in the posterior rim of the tectum. As shown in other species, goldfish adapt rapidly to repeated natural-looming stimulation (Marquez-Legorreta et al., 2022; Fotowat and Engert, 2023). Indeed, in previous behavioral experiments we presented looming stimuli with intertrial intervals (ITI) of about 4-5 minutes to reduce such adaptation (Preuss et al., 2006; Otero Coronel et al., 2020; Martorell and Medan, 2022). However, ITI of 4-5 min are prohibitively long for steady intracellular recordings. Considering these restrictions, we used tectal stimuli (that bypass the retina) at an ITI of 30 s which does not produce adaptation. This tectal stimulation results in depolarization responses in the ventral ('visual') dendrite of the M-cell that are qualitatively and quantitatively similar to those elicited by visual looming stimuli. While this approach bypasses retinal and tectal processing of visual inputs, it is important to note that the tectum also integrates multisensory inputs, including from the thalamus and other sensory pathways such as the auditory and vestibular systems (Bastian 1982, Fame et al., 2006, Kardamakis et al., 2016, Thompson et al., 2016, Poulson et al., 2021). As a result, tectal stimulation is likely to recruit projections that are predominantly, but not exclusively, visual. Nonetheless, tectal afferents reach the distal ventral dendrite of the M-cell and produce non-adapting synaptic responses that retain key characteristics of looming responses such as fast PSPs riding on top of a ramped depolarization (Preuss et al., 2006; Szabo et al., 2006; Medan and Preuss, 2014; Medan et al., 2017, Zottoli et al.,1987) (Figure 1A). M-cell somatic responses reach a plateau after 30-100 ms and decay to resting values 200-300 ms after the end of the tectal train. To characterize how the M-cell responses depend on the frequency and duration of the stimulation trains in the tectum, we recorded responses to 60-Hz trains that varied in duration (Figure 1A-B, N=18), and 100-ms tectal trains that varied in pulse frequency (Figure 1C-D, N=11). The responses to both sets of trains exhibited complex temporal dynamics with a tonic component that progressively builds during the train and a fast phasic component after each pulse (Figure 1A').

Increasing the duration of the 60-Hz trains drove stronger tectal responses due to the increase of the tonic component of the response while the phasic response remained unchanged (ANOVA, tonic: $F(3, 40)=37.29$, $p<0.0001$, phasic: $F(3,40)=0.58$, $p= 0.6311$, Figure 1B). Increasing the frequency of the

100-ms stimulation trains also drove stronger tectal responses due to a large increase in the tonic component (ANOVA, tonic: $F(3, 30)=12.29$, $p<0.0001$). However, increasing the tectal stimulus frequency produced a significant reduction in the amplitude of the phasic component (ANOVA, phasic: $F(3, 30)=11.29$, $p<0.0001$, Figure 1D). Comparing the stimulus trains of variable duration and frequency reveals that modifying the duration of the 60-Hz trains or the frequency of 100-ms trains is similarly effective in tuning the magnitude of the responses. Increasing the duration of a 60 Hz from 33 to 200 ms produced a 45% increase in the total response amplitude (phasic + tonic) while increasing the frequency from 30 to 200 Hz produced a 50% increase in the response amplitude (Figures 1 B, D). Since multimodal integration is known to depend on the strength of the unimodal components (Stanford et al., 2005; Martorell and Medan, 2022), in the following multimodal experiments we leveraged this characterization to generate tectal stimuli of variable strength and dynamics. Although both the 60-Hz trains of variable duration and the 100-ms trains of variable frequency evoked responses of similar total amplitude, we decided to include both sets of trains in our multisensory stimuli to determine whether any detected effect depended on the temporal structure of the stimulus or the ratio of phasic-to-tonic responses.

MULTISENSORY ENHANCEMENT IN THE MAUTHNER CELL

Abrupt sound stimuli have been extensively used to trigger the short latency escape responses initiated by firing of the M-cell (Eaton et al., 1977; Burgess and Granato, 2007; Neumeister et al., 2008; Weiss et al., 2009; Zheng and Schmid, 2023). Acoustic stimulation produces a complex response in the M-cell which is composed of a fast EPSP superimposed on a depolarizing envelope termed slow EPSP (Szabo et al., 2006). The fast EPSP is composed of fast electrical coupling potentials resulting from firing of the 8th nerve auditory afferences that synapse the distal end of the lateral dendrite of the M-cell (club endings) (Pereda et al., 2004; Szabo et al., 2007). In contrast, the slow EPSP is originated by chemical (glutamatergic) synaptic contacts on the soma and proximal dendrite conveying information from inner hear endorgans and it has been shown that it mostly carries information on stimulus intensity (Szabo et al., 2006). Although the M-cell is known to respond to stimuli of different modalities, there are no reports on how it combines and integrates information when auditory and tectal sources are co-presented. To determine whether multisensory enhancement occurs in the M-cell, we recorded somatic responses to an auditory pip (unisensory auditory, A), a tectal stimulation train (unisensory tectal, T), and their combination (multisensory audiotectal, M) (Figure 2A, E).

Increasing the duration of the 60-Hz tectal train positively modulated the multisensory responses (amplitudes ranging from 3.08 ± 0.84 mV to 5.29 ± 1.64 mV, N=17, n=47; LM: evoked depolarization

~ tectal duration, F(1,45)=17,39, p=0.0001, Figure 2B). We then compared the multisensory responses to their unisensory counterparts. When M responses were normalized to the most effective unisensory response, multisensory stimuli yielded MSI/Max indices that ranged from 1.48 to 1.53 for all stimulus durations (Wilcoxon single sample test mu=1, alternative mu≠1, p<0.001 for all stimulus durations, Figure 2C), indicating a significant multisensory enhancement of the response. When the M response was normalized to the sum of both unisensory responses, the MSI/Sum indices were lower than 1 (i.e. sublinear integration, Wilcoxon single sample test mu=1, alternative mu≠1, p<0.01) for all cases except for the briefest tectal stimulus, for which the MSI/Sum index was 1.06 (i.e. linear integration, Wilcoxon single sample test mu=1, alternative mu≠1, p<0.0676, Figure 2D).

Increasing the frequency of a 100-ms tectal train (Figure 2E) was not as effective in modulating the multisensory responses (LM: evoked depolarization ~ tectal frequency, F(1,39)=3.96, p=0.0535, Figure 2F). However, the M responses still exhibited MSI/Max indices that ranged 1.43-1.53 when compared to the largest unimodal stimulus (Figure 2G) indicating that a 100 ms tectal train (irrespective of its frequency) significantly enhances the M-cell response. The MSI/Sum of these M responses ranged 0.82 to 0.86 showing a similar sublinear integration to that of the multisensory stimuli with the longer 60-Hz trains (Wilcoxon single sample test mu=1, alternative mu≠1, all p≤0.01, Figure 2H). Neither MSI/Max or MSI/Sum showed a significant dependency with tectal frequency (LM: MSI/Max ~ tectal frequency, F(1,39)=0.02, p=0.882, MSI/Sum ~ tectal frequency, F(1,39)=0.49, p=0.487).

Overall, these results show that, in all cases, combining an auditory pip with a preceding tectal pulse enhances the M-cell response by about 50%. This multisensory enhancement does not show a strong modulation by the duration or frequency of the tectal stimulus (Figure 2C, G). However, while most multisensory stimuli exhibited a sublinear integration, the multisensory stimulus with the shortest (and weakest) tectal component produced a linear **response (Figure 2B, D).**

TECTAL- AND AUDITORY-EVOKED FEEDFORWARD INHIBITIONS EXHIBIT DISTINCT TEMPORAL DYNAMICS

Both visual and auditory stimuli evoke feedforward inhibition (FFI) at the perisomatic region of the M-cell through a population of inhibitory interneurons which open chloride channels that produce shunting of the postsynaptic currents (Diamond et al., 1973; Zottoli et al., 1987; Koyama et al., 2011; Tabor et al., 2018). This FFI restricts the temporal window of sensory excitation to terminate the excitatory signal. In combination with passive membrane decay, an increase in FFI will further narrow

the window for temporal integration. Conversely, a decrease in FFI would increase the lingering depolarization of a response produced by a previous stimulus, and thus extend the temporal integration window. These differences in the strength or temporal dynamics between visual and auditory evoked FFI may affect multisensory integration (Felch et al., 2016). We used a single auditory pip and a brief tectal train as "conditioning" stimuli of similar strength, which evoked comparable peak depolarizations in the M-cell (~5 mV) (Figure 3A). Peak FFI inhibition induced by auditory and tectal stimulation showed similar amplitude (Figure 3B, auditory vs. tectal %SI: 13.65 ± 4.74 vs. 14.55 ± 7.50; Kruskal-Wallis chi-squared (1)= 0.01, p = 0.9066, N=19) with peak inhibition at the same time (auditory vs. tectal time (ms) of maximum %SI: 9.04 ± 3.93 vs. 8.85 ± 6.54; Kruskal-Wallis chi-squared(1)= 0.30, p = 0.5838, Figure 3C, N=19). In a subset of experiments (N = 7), both auditory and tectal FFI were evaluated sequentially in the same cell and same recording site which allowed us to have an accurate estimate of the inhibition triggered by each sensory modality (Figure 3D). Although the maximum level of inhibition was comparable and was reached in a similar time, recovery from inhibition was much faster for tectal than for auditory FFI. Tectal FFI decayed to 50% of its peak in 8 ms, compared to 30 ms for the auditory FFI (Kruskal-Wallis chi-squared (1)= 5.97, p =0.0145, Figure 3E). In addition, the area under the curve for auditory FFI was almost 3 times greater than for tectal FFI (502 vs. 176 %*ms, respectively, Kruskal-Wallis chi-squared (1)= 5.58, p = 0.0181, Figure 3F).

These results highlight the key role of the temporal dynamics of the inhibition that reaches the M-cell and which in turn will affect integration in the M-cell. Moreover, these results show that auditory stimuli trigger more prolonged inhibition than tectal stimuli of similar amplitude and decay time. The short-lived FFI that follows tectal stimulation suggests that multiple trains or waves of tectal inputs are more likely to be integrated and summed than multiple sounds. This goes in line with the duration of visual looms that are most effective in triggering the M-cell and eliciting visual C-start escapes (Preuss et al., 2006; Temizer et al., 2015). Differences on the decay rate of inhibition produced by brief tectal or auditory stimuli could affect integration of pairs of brief sensory stimuli depending on their sequence and their timing, which is explored in the next section.

STIMULUS TEMPORAL ORDER AND MODALITY AFFECT STIMULI INTEGRATION

There are several anatomical and functional differences in the pathways followed by auditory and visual inputs that eventually reach the M-cell soma. First, auditory inputs from the 8th nerve reach the distal lateral dendrite of the M-cell through a disynaptic (≈2 ms) pathway followed by slower inputs from glutamatergic synaptic contacts on the soma and proximal dendrite**.** Visual inputs reach the ventral dendrite after a polysynaptic (≈20 ms) pathway that includes the optic tectum (Zottoli et

al., 1987; Szabo et al., 2006). Second, M-cell dendritic characteristics determine modality specific filtering differences resulting in stronger attenuation of visual than auditory signals (Medan et al., 2017). For auditory stimuli, it has been reported that a sound pip that precedes by 20-150 ms a second sound reduces the M-cell response to the second sound, a phenomenon known as auditory prepulse inhibition (Neumeister et al., 2008; Curtin and Preuss, 2015; Tabor et al., 2018). However, it is unclear whether a similar inhibitory integration would hold true for cross-modal and tectal-tectal interactions, since auditory and visual inputs travel through distinct and separated pathways and undergo different filtering.

To investigate the role of input modality on M-cell integration we used pairs of similarly brief (~10 ms) auditory pips and tectal pulses 50 ms apart with in all possible sequences, including unisensory combinations (AA, TT) and multisensory combinations (AT, TA, Figure 4, N= 29, n= 50). We decided to use a 50 ms interval because it was observed to be a period after which the tectal FFI had returned to baseline values, while the auditory FFI remained at about 4%. The amplitude of the tectal stimulation pulse was chosen so that the M-cell responses to the tectal and auditory stimuli were of similar magnitude (4-8 mV). The initial response to the first stimulus (S1, auditory in the example shown in Figure 4A, top trace) decayed passively over the course of 50 ms, and at that point the second stimulus was presented (S2, tectal in the example shown if Figure 4A, bottom trace). The mean lingering depolarization remaining immediately before the second stimulus was delivered (Figure 4A, top trace, pink bar) was slightly larger for the evoked auditory pip than for the tectal stimulus (Figure 4B, A: 1.48 ± 0.79mV vs. T: 0.95 ± 0.50mV, Kruskal-Wallis rank sum test (1) = 5.5173, p = 0.0188).

We next calculated the integration indices of the four possible combinations of uni and multisensory pairs (AA, AT, TA, TT). For that, we measured the depolarization in A-only or T-only trials in 12-ms windows. These windows started either 50 ms after stimulus onset to account for the contribution of the first stimulus, S1 (Figure 4A, Resp1, orange area of top trace), or immediately after stimulus presentation to account for the contribution of the second stimulus, S2 (Figure 4A, Resp2, green area of middle trace). Then, we measured the response for pairs of stimuli in a 12-ms window after the presentation of S2 (Figure 4A, Resp(1+2), bottom trace). Finally, we calculated the integration for each type of uni (AA and TT) or multisensory stimuli (AT and TA) defining a “S1-S2 Integration Index” as S1-S2 Int./Sum= Resp(1+2)/(Resp1 + Resp2)). Note that for multisensory trials (i.e. AT or TA), this metric is equivalent to the MSI/Sum index, except for a 50-ms temporal offset in the presentation and quantification of the first stimulus.

In the AA trials (N=21) we observed an inhibitory integration (S1-S2 Int./Sum < 1, two-sided Wilcoxon rank test, p<0.0001) with the first auditory pip reducing the amplitude expected for the second pip by 42%, as others have previously described (Neumeister et al., 2008; Curtin and Preuss, 2015; Tabor et al., 2018). The AT combination also showed sublinear integration (S1-S2 Int./Sum < 1, two-sided Wilcoxon rank test, p = 0.0078) while the TT and TA combinations showed linear integration (S1-S2 Int./Sum =1, two-sided Wilcoxon rank test, VA: p = 0.0681, VV: p = 0.9453, Figure 4C). The inhibitory effect in the AA combination was significantly larger than for the AT combination (Figure 4C, 1w-ANOVA, F=38.34, p<0.0001).

MULTISENSORY INTEGRATION IN THE MAUTHNER CELL SHOWS INVERSE EFFECTIVENESS

The principle of inverse effectiveness states that the effects of multisensory integration are typically larger when the components of a multisensory stimulus are weak. Throughout our experiments, we only observed linear integration of multisensory stimuli when presenting single tectal pulses (Figure 2C, 1ms tectal), or brief (~10 ms) trains (Figure 4, AT – TA), and observed sublinear integration for multimodal stimuli with longer tectal trains (Figure 2D-H). However, these results represent the average MSI for each group for a specific set of experimental conditions and effectively simplify the diverse range of responses across trials, experimental conditions, and fish. To compare the overall dependence of the multisensory enhancement on the strength of sensory inputs, we pooled the multisensory integration indexes for experiments irrespective of sequence of stimuli (AT and TA, N=18, n=174), tectal train duration (from a single 1-ms tectal pulse to a 200-ms train) and frequency (from a single pulse to 1000Hz) (Figure 5A, MSI/Max and B, MSI/Sum). We found a significant inverse correlation between the magnitude of the multisensory enhancement and the magnitude of the unisensory components (MSI/Max, LM, F(1,172): 28.17, p<0.0001; MSI/Sum, LM, F(1,172): 67.33, p<0.0001). This result parallels the inverse effectiveness reported at the behavioral level in goldfish (McIntyre and Preuss, 2019; Martorell and Medan, 2022), confirming that the relative multisensory enhancement obtained by combining two inputs is proportionally higher when the stimuli are weak. Combinations of weak stimuli (<2.5mV, Figure 5B) produce supralinear multisensory responses that are between 50-100% stronger than the most effective unisensory stimulus (Figure 5A). Noteworthy, these results provide robust evidence that in the escape network of fish, inverse effectiveness of multisensory integration is implemented, at least, at the single (Mauthner) cell level.

DISCUSSION

The Mauthner-cell system triggers a behavior of vital importance: escaping from predators. A combination of fast afferent circuits, synaptic specialization, special intrinsic properties and topology of the M-cell contribute in concert to a fast startle escape response (Eaton et al., 1991; Korn and Faber, 2005). Here we show that the M-cell incorporates multisensory information to enhance its responses and characterize how the integration of multiple stimuli is affected by the modality, spatial source, temporal structure, temporal order, and intensity of the stimuli. Although multisensory enhancement has been previously described in different neural populations and across a wide range of species, it was unclear whether the activity of these neurons was necessary, sufficient, or even influenced the execution of behavioral responses to multisensory stimuli. In contrast to other known multisensory structures of vertebrates multisensory integration in the M-cell has an unequivocal function in fish behavior and survival, as it directly determines whether and when a C-start is triggered (McIntyre and Preuss, 2019; Martorell and Medan, 2022) .

Different factors differentially affect the summation and integration of auditory and visual inputs to the M-cell. First, sensory inputs are subject to different passive decays depending on the site of the dendritic arbor at which they arrive. Auditory inputs reach the M-cell distal lateral dendrite through dense mixed electrical and chemical synapses driven through the posterior 8th-nerve afferents and the proximal dendrite through indirect glutamatergic inputs conveying information from inner ear endorgans (Szabo et al., 2006, 2007). In contrast, visual inputs arriving to the ventral dendrite establish synapses that do not show additional specializations as the club endings (Zottoli et al., 1987; Cachope et al., 2007; Szabo et al., 2007). Second, the geometrical properties of the M-cell lateral and ventral dendrites (length and tapering) impose different filters on the input signal which determine a stronger spatial decay for visual than for auditory signals (Medan et al., 2017). Third, as excitatory (and inhibitory) signals reach the soma, the active ion conductances decrease the membrane resistance and impact the response to following signals (Hodgkin, 1947). Finally, the magnitude and dynamics of the stimuli will also affect integration. Both abrupt auditory pips and longer lasting auditory looms generate fast EPSPs that depend on the stimulus frequency and a depolarizing envelope proportional to the stimulus amplitude (Szabo et al., 2006) that slowly decays to baseline (Figure 4). Although the pathways for auditory and visual inputs are completely different, tectal responses also consist of fast peaks that track stimulus frequency and a tonic depolarizing envelope proportional both to stimulus duration and frequency (Figure 1) that also decays slowly (Figure 4).

These temporal dynamics of the responses modulate the effective multisensory integration in the M-cell soma, which emerges as a complex, nonlinear interaction between “positive” (input strength and summation, voltage dependent depolarizing conductances) and “negative” (temporal and spatial decay, feedforward inhibition, and depolarization-induced decrease in input resistance) contributions. These factors likely influence integration in any multisensory neuron. However, the accumulated knowledge on the presynaptic pathways and the intrinsic mechanisms operating in the M-cell combined with its functional role in commanding the initiation of the C-start response makes this neuron a unique model for analyzing multisensory integration in a single identifiable neuron.

We have previously shown that fish exhibit a behavioral multisensory enhancement of the C-start escape response for audiovisual stimuli, and that this effect is reduced when increasing the salience of the unisensory stimuli (Martorell and Medan, 2022). Therefore, one of our goals here was to investigate if the inverse effectiveness principle observed behaviorally had its correlation in integration processes taking place in the M-cell. Paralleling our previous behavioral results, here we show through intracellular recordings that the response evoked by an auditory pip can be increased by about 50% when it is preceded by a tectal stimulus (Figure 2C, G). This enhancement was not affected by relatively large changes in stimulus frequency. The plateau in the tonic depolarization observed 30-50 ms after a sustained stimulus (Figure 1A) combined with the low-pass filtering properties of the membrane could be responsible for the lack of frequency effects. These two mechanisms point to the M-cell role as a “sudden” stimulus detector rather than a precise coder of sensory stimulus properties.

When we combined a tectal train with an auditory pip to obtain a multisensory stimulus, the response was smaller than the sum of the evoked depolarization of the two components (Figures 2D, H). This sublinear effect was expected in the case of passive integration, since cellular biophysics predict a sublinear integration of subthreshold inputs due to a reduction in the driving force of sodium and the aperture of ion channels that reduce the membrane resistance. Noteworthy, action potentials are all-or-nothing events, so the effects when the membrane potential is close to the threshold, sublinear summation can determine that an otherwise silent neuron fires an AP (Figure 5C). Therefore, a weak (subthreshold) auditory pip combined by a weak visual stimulus in close temporal association might be sufficient for triggering an escape response. Indeed, analysis of 60 M-cells tested with A, T and M stimuli showed that auditory stimuli evoked firing in 5% of cells, tectal stimuli in 6.7% of cells but almost 12% of M-cells fired in response to multisensory stimuli. Even though these results are probably an underestimation of actual firing probabilities due to anesthesia

and paralyzing agents, they provide a mechanistic support to our previous behavioral observations (Martorell and Medan, 2022).

Importantly, for the weakest multisensory stimuli the M-cell response deviated from this sublinear integration (Figures 2C and 5A). When the sum of unisensory components is less than 2.5 mV (essentially a single tectal stimulus immediately followed by a single auditory pip) summation is linear (Figure 2D and 5A). This suggests the existence of one or more active mechanism/s of multisensory integration upstream of the M-cell soma, potentially through a presynaptic neuron that also receives audiovisual inputs and projects to the M-cell or locally at the level of the dendritic tree of the M-cell. Moreover, previous work has described the M-cell membrane non-linearities in the lateral and ventral dendrites which progressively increase M-cell excitability for depolarizations above 5 mV (Faber and Korn, 1986; Medan et al., 2017). Such nonlinear properties might enhance multisensory integration of weak stimuli (Martorell and Medan, 2022) providing a cellular mechanism for the principle of inverse effectiveness of multisensory integration.

The temporal structure of the multisensory stimuli is crucial to allow the animal to effectively "bind" or associate both signals as coming from a single source (Stein and Stanford, 2008). In the M-cell, this translates into the time window where the effect on the membrane voltage (excitatory or inhibitory) persists. Here, we found that a delay of 50 ms between the components of a low-amplitude multisensory stimuli result in a linear summation of the signals (Figure 4C) and that the temporal order of the components produces a slight effect in the integration (Figure 4C, AT vs. TA) (Felch et al., 2016). As it has been previously suggested, the lengthy decay of the slow EPSP of the auditory pip (or the tonic component of the tectal train) probably contributed to relax the requirement for coincident inputs, effectively broadening the temporal window of integration (Szabo et al., 2006). On the other hand, the integration of unisensory stimuli was dependent on the modality of the stimuli: two tectal (TT) stimuli summed linearly while two auditory (AA) stimuli summed sublinearly (Figure 4C). This difference might be due to differences in both the presynaptic networks that mediate PPI (Tabor et al., 2018) and in the temporal decay of auditory and tectally evoked FFI (Figure 3D). Auditory stimuli produce a longer-lasting inhibition than tectal stimuli of similar strength (Figure 3F) and while tectal inhibition is almost extinct 50 ms after a tectal stimulus, auditory inhibition stabilizes at around 50% of the maximum inhibitory effect in a time window of 30 to 70 ms after an auditory stimulus (Figure 3E). Interestingly, the integration of AT stimuli was smaller than that of TA, supporting a differential cross-modal and intra-modal integration of the excitatory or inhibitory components (Figure 4C). Another factor that could be contributing to the differential integration between AA and AT stimuli is that FFI inhibition is likely to be heterogeneously spread in the perisomatic area around the M-cell. If

auditory stimulation recruits inhibitory PHP neurons that target the proximal lateral dendrite of the M-cell, a subsequent sensory input propagating along the lateral dendrite (i.e, auditory input) would suffer stronger attenuation than one reaching the soma through the ventral dendrite (i.e., tectal input). However, specific studies are required to test this hypothesis as it is still unclear if auditory and tectal afferent fibers synapse the same or different sets of inhibitory neurons and which is the spatial distribution of those inhibitory contacts. Additionally, presynaptic elements could also contribute to the asymmetry in unimodal auditory (AA) vs. unimodal tectal (TT) or multisensory processing. A subset of glutamatergic Gsx1 neurons located in rhombomere 4 have been shown to mediate M-cell auditory presynaptic inhibition (Tabor et al., 2018). These neurons produce presynaptic inhibition of 8th nerve auditory fibers adjacent to the distal portion of the M-cell lateral dendrite but leave unaffected the ventral dendrite. This mechanism could therefore affect the processing of pairs of sensory signals that initiate with an auditory component (AA, AT) and leave the integration of tectal or multisensory stimuli unaffected.

ACKNOWLEDGEMENTS

This work was supported by PICT 2012-1578 and PICT 2017-0007, FONCYT-ANPCYT (VM), PIP 11220130100729CO (VM), UBACyT 20020130300008BA (VM), Thalmann Program, University of Buenos Aires (VM) SOC was supported by undergraduate fellowships from the National Interuniversity Council and University of Buenos Aires. The authors thank Dr. Lidia Szczupak and members of the Medan lab for discussion and for reading previous versions of this manuscript. The current address of SOC is at The Rockefeller University, New York, NY, USA (10065).

AUTHOR CONTRIBUTIONS

SOC, TP and VM conceived the research. SOC and VM performed experiments and analyzed the data. SOC and VM wrote the manuscript.

REFERENCES

Bastian J. (1982) Vision and electroreception: Integration of sensory information in the optic tectum of the weakly electric fishApteronotus albifrons . J. Comp. Physiol. 147, 287–297.

Burgess HA, Granato M (2007) Sensorimotor gating in larval zebrafish. J Neurosci 27:4984–4994.

Cachope R, Mackie K, Triller A, O'Brien J, Pereda AE (2007) Potentiation of electrical and chemical synaptic transmission mediated by endocannabinoids. Neuron 56:1034–1047.

Canfield JG (2006) Functional evidence for visuospatial coding in the Mauthner neuron. Brain Behav Evol 67:188–202.

Cordova MS, Braun CB (2007) The use of anesthesia during evoked potential audiometry in goldfish (Carassius auratus). Brain Res 1153:78–83.

Curtin PCP, Preuss T (2015) Glycine and GABAA receptors mediate tonic and phasic inhibitory processes that contribute to prepulse inhibition in the goldfish startle network. Front Neural Circuits 9:12.

Dean P, Redgrave P, Westby GWM (1989) Event or emergency? Two response systems in the mammalian superior colliculus. Trends Neurosci 12:137–147.

Diamond J, Roper S, Yasargil GM (1973) The membrane effects, and sensitivity to strychnine, of neural inhibition of the Mauthner cell, and its inhibition by glycine and GABA. J Physiol 232:87–111.

Eaton RC, Bombardieri RA, Meyer DL (1977) The Mauthner-initiated startle response in teleost fish. J Exp Biol 66:65–81.

Eaton RC, DiDomenico R, Nissanov J (1991) Role of the Mauthner cell in sensorimotor integration by the brain stem escape network. Brain Behav Evol 37:272–285.

Faber DS, Korn H (1982) Transmission at a central inhibitory synapse. I. Magnitude of unitary postsynaptic conductance change and kinetics of channel activation. J Neurophysiol 48:654–678.

Faber DS, Korn H (1986) Instantaneous inward rectification in the Mauthner cell: a postsynaptic booster for excitatory inputs. Neuroscience 19:1037–1043.

Faber DS, Korn H (1989) Electrical field effects: their relevance in central neural networks. Physiol Rev 69:821–863.

Fame RM, Brajon C, Ghysen A (2006) Second-order projection from the posterior lateral line in the early zebrafish brain. Neural Dev 1, 4.

Felch DL, Khakhalin AS, Aizenman CD (2016) Multisensory integration in the developing tectum is constrained by the balance of excitation and inhibition. eLife 5:e15600.

Finger TE, Tong S-L (1984) Central organization of eighth nerve and mechanosensory lateral line systems in the brainstem of ictalurid catfish. J. Comp. Neurol., 229: 129-151.

Fotowat H, Engert F (2023) Neural circuits underlying habituation of visually evoked escape behaviors in larval zebrafish Kawakami K, Moore T, eds. eLife 12:e82916.

Furshpan EJ, Furukawa T (1962) Intracellular and extracellular responses of the several regions of the Mauthner cell of the goldfish. J Neurophysiol 25:732–771.

Furukawa T (1966) Synaptic interaction at the mauthner cell of goldfish. Prog Brain Res 21:44–70.

Gil-Guevara O, Bernal HA, Riveros AJ (2022) Honey bees respond to multimodal stimuli following the principle of inverse effectiveness. J Exp Biol 225:jeb243832.

Hodgkin AL (1947) The membrane resistance of a non-medullated nerve fibre. J Physiol 106:305–318.

Kadunce DC, Vaughan JW, Wallace MT, Stein BE (2001) The influence of visual and auditory receptive field organization on multisensory integration in the superior colliculus. Exp Brain Res 139:303–310.

Kardamakis AA, Pérez-Fernández P, Grillner S (2016) Spatiotemporal interplay between multisensory excitation and recruited inhibition in the lamprey optic tectum. eLife 5:e16472.

Korn H, Faber DS (2005) The Mauthner cell half a century later: a neurobiological model for decision-making? Neuron 47:13–28.

Koyama M, Kinkhabwala A, Satou C, Higashijima S, Fetcho J (2011) Mapping a sensory-motor network onto a structural and functional ground plan in the hindbrain. Proc Natl Acad Sci U S A 108:1170–1175.

Marquez-Legorreta E, Constantin L, Piber M, Favre-Bulle IA, Taylor MA, Blevins AS, Giacomotto J, Bassett DS, Vanwalleghem GC, Scott EK (2022) Brain-wide visual habituation networks in wild type and fmr1 zebrafish. Nat Commun 13:895.

Martorell N, Medan V (2022) Audiovisual integration in the Mauthner cell enhances escape probability and reduces response latency. Sci Rep 12:1097.

McIntyre C, Preuss T (2019) Influence of Stimulus Intensity on Multimodal Integration in the Startle Escape System of Goldfish. Front Neural Circuits 13:7.

Medan V, Mäki-Marttunen T, Sztarker J, Preuss T (2017) Differential processing in modality-specific Mauthner cell dendrites. J Physiol. 596(4):667-689.

Medan V, Preuss T (2014) The Mauthner-cell circuit of fish as a model system for startle plasticity. J Physiol-Paris 108:129–140.

Meredith MA, Stein BE (1983) Interactions among converging sensory inputs in the superior colliculus. Science 221:389–391.

Meredith MA, Stein BE (1996) Spatial determinants of multisensory integration in cat superior colliculus neurons. J Neurophysiol 75:1843–1857.

Metaxakis A, Petratou D, Tavernarakis N (2018) Multimodal sensory processing in Caenorhabditis elegans. Open Biol 8:180049.

Neumeister H, Szabo TM, Preuss T (2008) Behavioral and physiological characterization of sensorimotor gating in the goldfish startle response. J Neurophysiol 99:1493–1502.

Otero Coronel S, Martorell N, Beron de Astrada M, Medan V (2020) Stimulus Contrast Information Modulates Sensorimotor Decision Making in Goldfish. Front Neural Circuits 14:23.

Palmer LM, Mensinger AF (2004) Effect of the anesthetic tricaine (MS-222) on nerve activity in the anterior lateral line of the oyster toadfish, Opsanus tau. J Neurophysiol 92:1034–1041.

Pereda AE, Rash JE, Nagy JI, Bennett MVL (2004) Dynamics of electrical transmission at club endings on the Mauthner cells. Brain Res Brain Res Rev 47:227–244.

Poulsen RE, Scholz LA, Constantin L, Favre-Bulle I, Vanwalleghem GC, Scott EK (2021) Broad frequency sensitivity and complex neural coding in the larval zebrafish auditory system. Curr Biol. 31(9):1977-1987.e4.

Preuss T, Faber DS (2003) Central cellular mechanisms underlying temperature-dependent changes in the goldfish startle-escape behavior. J Neurosci 23:5617–5626.

Preuss T, Osei-Bonsu PE, Weiss SA, Wang C, Faber DS (2006) Neural representation of object approach in a decision-making motor circuit. J Neurosci Off J Soc Neurosci 26:3454–3464.

Rowland BA, Quessy S, Stanford TR, Stein BE (2007) Multisensory integration shortens physiological response latencies. J Neurosci Off J Soc Neurosci 27:5879–5884.

Stanford TR, Quessy S, Stein BE (2005) Evaluating the Operations Underlying Multisensory Integration in the Cat Superior Colliculus. J Neurosci 25:6499–6508.

Stanford TR, Stein BE (2007) Superadditivity in multisensory integration: putting the computation in context. Neuroreport 18:787–792.

Stein BE, Stanford TR (2008) Multisensory integration: current issues from the perspective of the single neuron. Nat Rev Neurosci 9:255–266.

Szabo TM, McCormick CA, Faber DS (2007) Otolith endorgan input to the Mauthner neuron in the goldfish. J Comp Neurol 505:511–525.

Szabo TM, Weiss SA, Faber DS, Preuss T (2006) Representation of auditory signals in the M-cell: role of electrical synapses. J Neurophysiol 95:2617–2629.

Tabor KM, Smith TS, Brown M, Bergeron SA, Briggman KL, Burgess HA (2018) Presynaptic Inhibition Selectively Gates Auditory Transmission to the Brainstem Startle Circuit. Curr Biol CB 28:2527-2535.e8.

Temizer I, Donovan JC, Baier H, Semmelhack JL (2015) A Visual Pathway for Looming-Evoked Escape in Larval Zebrafish. Curr Biol CB 25:1823–1834.

Thompson AW, Vanwalleghem GC, Heap LA, Scott EK (2016) Functional Profiles of Visual-, Auditory-, and Water Flow-Responsive Neurons in the Zebrafish Tectum. Curr Biol 26(6): 743-754.

Wallace MT, Meredith MA, Stein BE (1998) Multisensory integration in the superior colliculus of the alert cat. J Neurophysiol 80:1006–1010.

Wei P, Liu N, Zhang Z, Liu X, Tang Y, He X, Wu B, Zhou Z, Liu Y, Li J, Zhang Y, Zhou X, Xu L, Chen L, Bi G, Hu X, Xu F, Wang L (2015) Processing of visually evoked innate fear by a non-canonical thalamic pathway. Nat Commun 6:6756.

Weiss SA, Preuss T, Faber DS (2009) Phase encoding in the Mauthner system: implications in left-right sound source discrimination. J Neurosci 29:3431–3441.

Weiss SA, Zottoli SJ, Do SC, Faber DS, Preuss T (2006) Correlation of C-start behaviors with neural activity recorded from the hindbrain in free-swimming goldfish (Carassius auratus). J Exp Biol 209:4788–4801.

Zheng A, Schmid S (2023) A review of the neural basis underlying the acoustic startle response with a focus on recent developments in mammals. Neurosci Biobehav Rev 148:105129.

Zhou G, Lane G, Noto T, Arabkheradmand G, Gottfried JA, Schuele SU, Rosenow JM, Olofsson JK, Wilson DA, Zelano C (2019) Human olfactory-auditory integration requires phase synchrony between sensory cortices. Nat Commun 10:1168.

Zottoli SJ (1977) Correlation of the startle reflex and Mauthner cell auditory responses in unrestrained goldfish. J Exp Biol 66:243–254.

Zottoli SJ, Hordes AR, Faber DS (1987) Localization of optic tectal input to the ventral dendrite of the goldfish Mauthner cell. Brain Res 401:113–121.

Zwaka H, McGinnis OJ, Pflitsch P, Prabha S, Mansinghka V, Engert F, Bolton AD (2022) Visual object detection biases escape trajectories following acoustic startle in larval zebrafish. Curr Biol 32:5116-5125.e3.

FIGURE LEGENDS

Figure 1. M-cell responses to tectal stimulation. A. M-cell responses to a 60 Hz tectal train of 200 ms were used to measure the evoked depolarization at 1, 33, 100 and 200 ms after stimulus onset during a 12-ms time window (colored vertical boxes). A´. Blue and orange bars in the trace show the tonic and phasic components of the response, respectively. The horizontal dotted lines indicate the baseline (bottom) and the potential before the last pulse for quantification of each component. B. Mean amplitude (± SEM) of the phasic (shades of orange) and tonic (shades of blue) components of tectal trains for the time windows described in A. C. M-cell responses to a 100 ms tectal pulse train of 30, 60, 100 or 200 Hz were recorded and quantified as in A, at the end of the pulse. D. Mean amplitude (± SEM) of the phasic (shades of orange) and tonic (shades of blue) components of 100-ms tectal trains of different frequency.

Figure 2. Multisensory integration in the M-cell. A. Diagram of stimulation (left) and response examples (right). The response examples correspond, to a single acoustic pulse (blue trace) and to their multisensory combination (purple). Below the traces diagram of the stimulation is shown in gray. B. Stacked bars comparing mean (± SEM) depolarization evoked by tectal trains of indicated duration (T, orange), auditory (A, blue) or their multisensory combination (purple). C. Boxplots showing the ratios between the multisensory responses and the maximum unisensory response (MSI/Max). D. Boxplots showing the ratios between the multisensory responses and the sum of its unisensory components (MSI/Sum). E-H. As in A-D but for 100 ms tectal trains of different frequencies.

Figure 3. Auditory and tectal FFI have different decay dynamics. A. Diagram of auditory or tectal feedforward inhibition circuits (center), and the quantification of sensory evoked shunting inhibition as a reduction of M-cell AP amplitude (left, auditory: shaded-blue area; right, tectal: shaded-red area) to a control AP (black trace). B-C. Boxplots of peak inhibition and time of peak inhibition triggered by acoustic or tectal stimuli. D. Mean (±SEM) FFI triggered by tectal and auditory inputs measured in the same M-cells at different time points between 0 and 70 ms post-stimulus. E. Boxplot of the time elapsed to 50% decay of peak FFI for the auditory (left) and tectal (right) stimuli. *p=0.0145. F. Area below the curve (0-70 ms) for the auditory (left) and tectal (right) stimuli. *p=0.0181.

Figure 4. Effect of stimulus sequence and modality on M-cell integration. A. Representative responses of one M-cell to two stimuli presented in different trials, or in the same trials with a 50 ms offset. The upper trace shows the M-cell response to an auditory stimulus (S1/A), middle trace corresponds to the response to a single tectal pulse (S2/T) and bottom trace shows the response to an A stimulus followed by a T stimulus 50 ms later. The area used to quantify each response is shaded in orange (Resp1), dark green (Resp2) or light green (Resp(1+2)) respectively. Schematics below each trace the order of stimuli and the area where responses were quantified. The pink bar indicates the time point at which the lingering depolarization of the first response was measured. Note that this analysis was performed for trials in which S1 and S2 could be either A or T, resulting in trials AA, TT, TA and AT sequences. B. Lingering depolarization after 50 ms of a single auditory pip or a short tectal train. *p=0.0188. C. Integration in the M-cell for pairs of uni- or multisensory stimuli with a 50 ms delay was calculated as the ratio: Resp (1+2) / (Resp1 + Resp2).

Figure 5. Multisensory integration of subthreshold unisensory stimuli. A. MSI/Max vs. the maximum unisensory response of different multisensory stimuli, irrespective of duration, frequency, or sequence of stimulation. B. Similar to A, but with the MSI/Sum instead vs. the sum of the unisensory responses.

Supplementary Figure 1. A-B. Representative recordings of left or right M-cell somatic responses to an electric stimulus train delivered to the left tectum (A) or to a short 200 Hz sound pip produced by a loudspeaker placed to the right side of the fish (B). The mean (of 3-5 repetitions) response is shown in solid color and the diagram of the tectal stimulus or the sound pip are shown below the traces. Dashed boxes indicate the 12-ms time windows following the stimulus where the responses were quantified. C-D. Boxplots showing the median, upper and lower quartiles and comparing the response to the same stimulus in the left or right M-cell in 9 fish for the tectal stimulus (C) and 11 fish for the auditory stimulus (D). Markers with the same color in left and right belong to pairs of M-cells of the same fish. No differences were found in the evoked response amplitude between the left and right M-cells or for tectal or auditory stimuli.

Figure 1

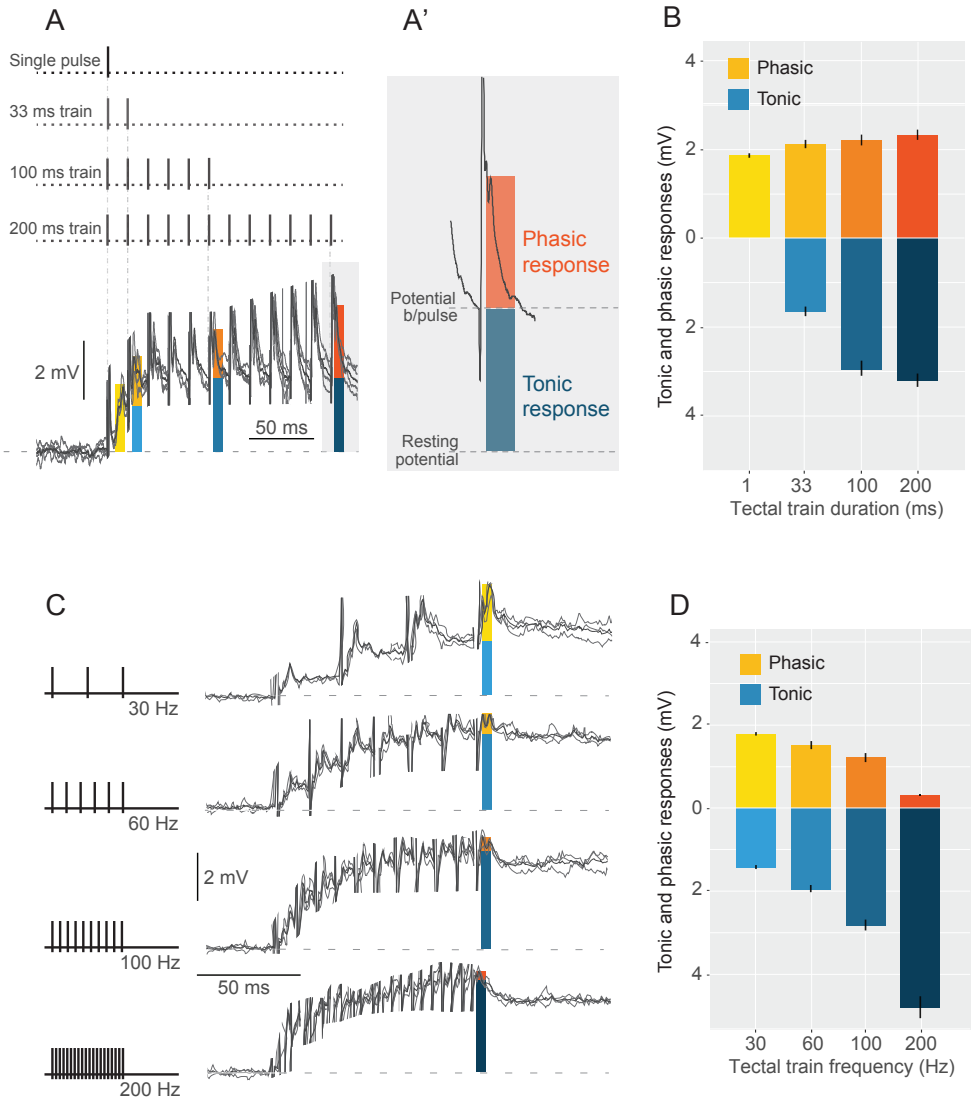

Figure 1. M-cell responses to tectal stimulation. A. M-cell responses to a 60 Hz tectal train of 200 ms were used to measure the evoked depolarization at 1, 33, 100 and 200 ms after stimulus onset during a 12-ms time window (colored vertical boxes). A´. Blue and orange bars in the trace show the tonic and phasic components of the response, respectively. The horizontal dotted lines indicate the baseline (bottom) and the potential before the last pulse for quantification of each component. B. Mean amplitude (± SEM) of the phasic (shades of orange) and tonic (shades of blue) components of tectal trains for the time windows described in A. C. M-cell responses to a 100 ms tectal pulse train of 30, 60, 100 or 200 Hz were recorded and quantified as in A, at the end of the pulse. D. Mean amplitude (± SEM) of the phasic (shades of orange) and tonic (shades of blue) components of 100-ms tectal trains of different frequency.

Figure 2

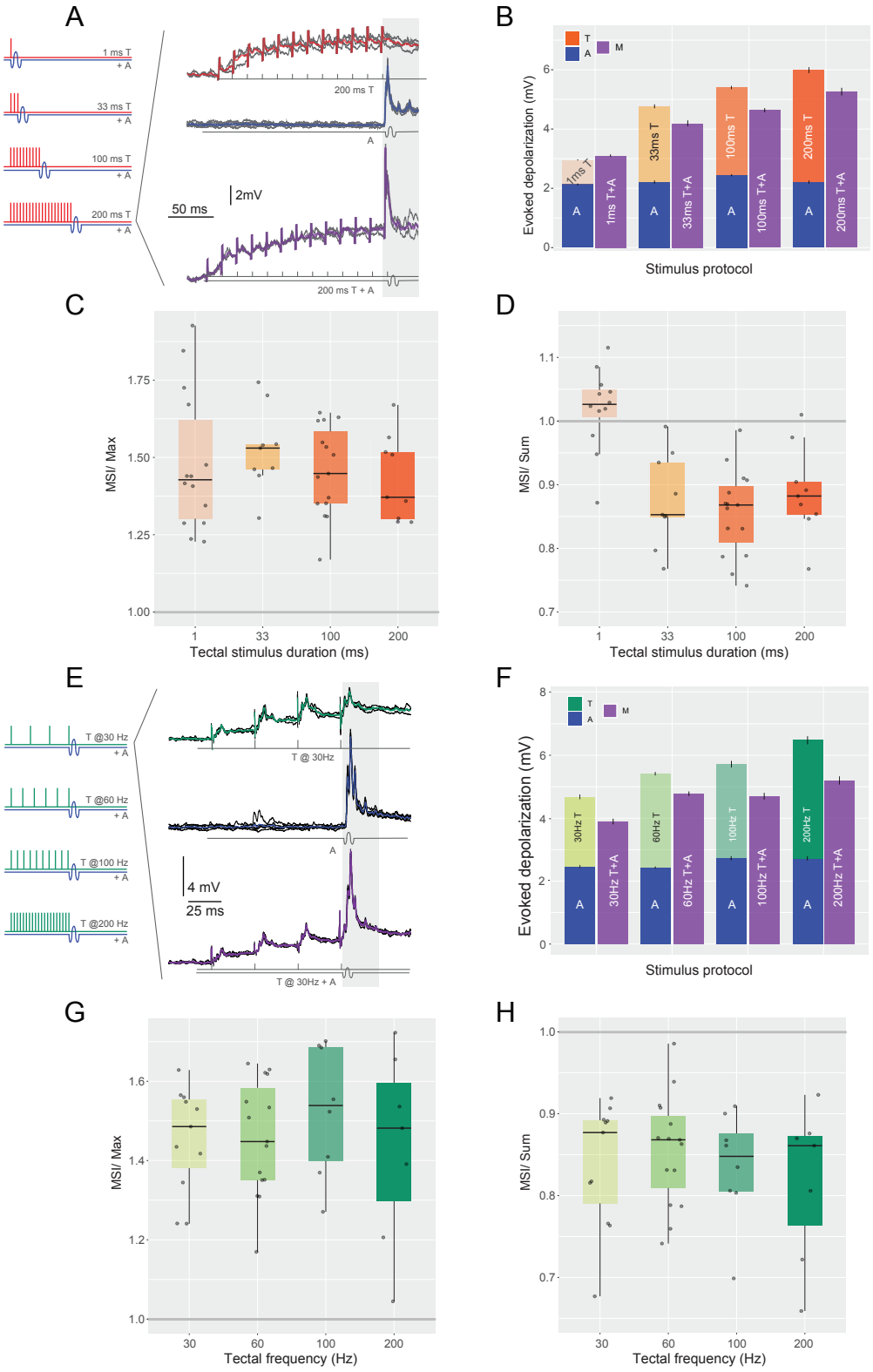

Figure 2. Multisensory integration in the M-cell. A. Diagram of stimulation (left) and response examples (right). The response examples correspond, to a single acoustic pulse (blue trace) and to their multisensory combination (purple). Below the traces diagram of the stimulation is shown in gray. B. Stacked bars comparing mean (± SEM) depolarization evoked by tectal trains of indicated duration (T, orange), auditory (A, blue) or their multisensory combination (purple). C. Boxplots showing the ratios between the multisensory responses and the maximum unisensory response (MSI/Max). D. Boxplots showing the ratios between the multisensory responses and the sum of its unisensory components (MSI/Sum). E-H. As in A-D but for 100 ms tectal trains of different frequencies.

Figure 3

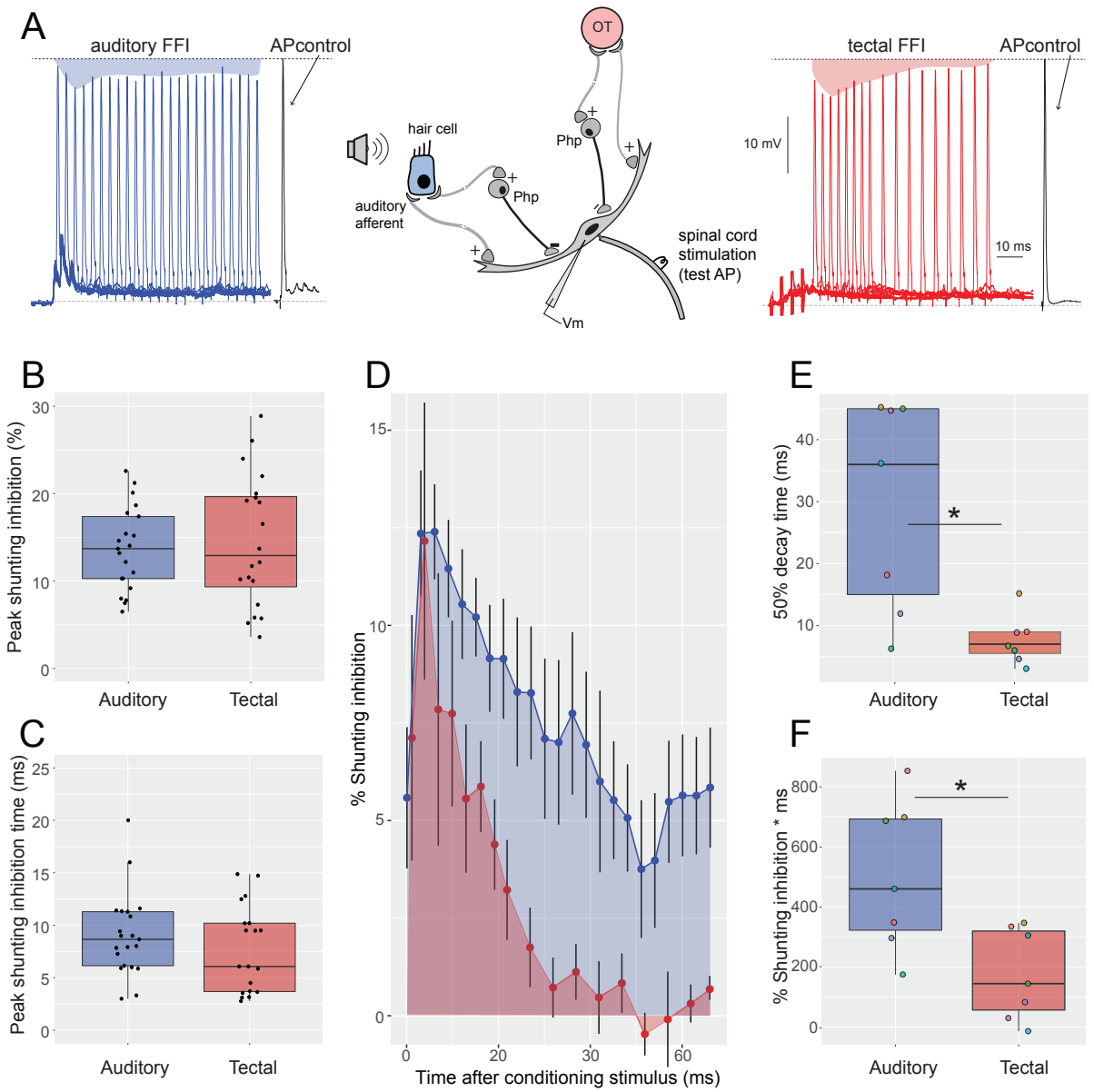

Figure 3. Auditory and tectal FFI have different decay dynamics. A. Diagram of auditory or tectal feedforward inhibition circuits (center), and the quantification of sensory evoked shunting inhibition as a reduction of M-cell AP amplitude (left, auditory: shaded-blue area; right, tectal: shaded-red area) to a control AP (black trace). B-C. Boxplots of peak inhibition and time of peak inhibition triggered by acoustic or tectal stimuli. D. Mean (±SEM) FFI triggered by tectal and auditory inputs measured in the same M-cells at different time points between 0 and 70 ms post-stimulus. E. Boxplot of the time elapsed to 50% decay of peak FFI for the auditory (left) and tectal (right) stimuli. *p=0.0145. F. Area below the curve (0-70 ms) for the auditory (left) and tectal (right) stimuli. *p=0.0181.

Figure 4

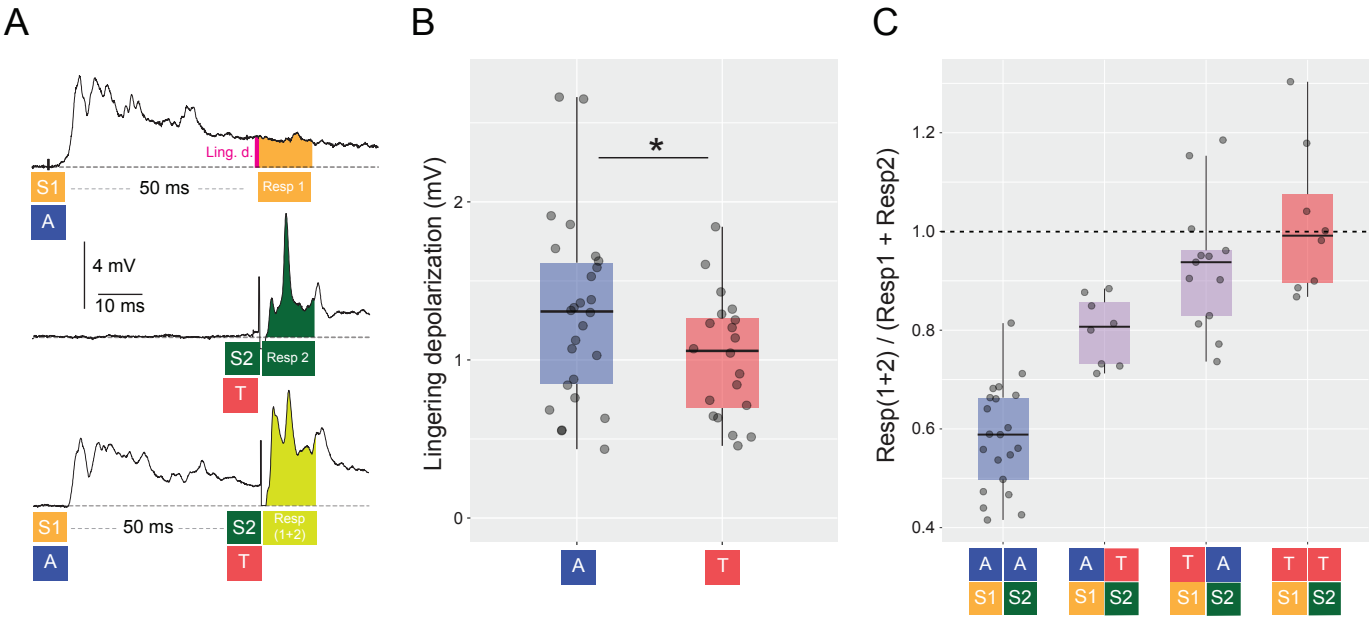

Figure 4. Effect of stimulus sequence and modality on M-cell integration. A. Representative responses of one M-cell to two stimuli presented in different trials, or in the same trials with a 50 ms offset. The upper trace shows the M-cell response to an auditory stimulus (S1/A), middle trace corresponds to the response to a single tectal pulse (S2/T) and bottom trace shows the response to an A stimulus followed by a T stimulus 50 ms later. The area used to quantify each response is shaded in orange (Resp1), dark green (Resp2) or light green (Resp(1+2)) respectively. Schematics below each trace the order of stimuli and the area where responses were quantified. The pink bar indicates the time point at which the lingering depolarization of the first response was measured. Note that this analysis was performed for trials in which S1 and S2 could be either A or T, resulting in trials AA, TT, TA and AT sequences. B. Lingering depolarization after 50 ms of a single auditory pip or a short tectal train. *p=0.0188. C. Integration in the M-cell for pairs of uni- or multisensory stimuli with a 50 ms delay was calculated as the ratio: Resp (1+2) / (Resp1 + Resp2).

Figure 5

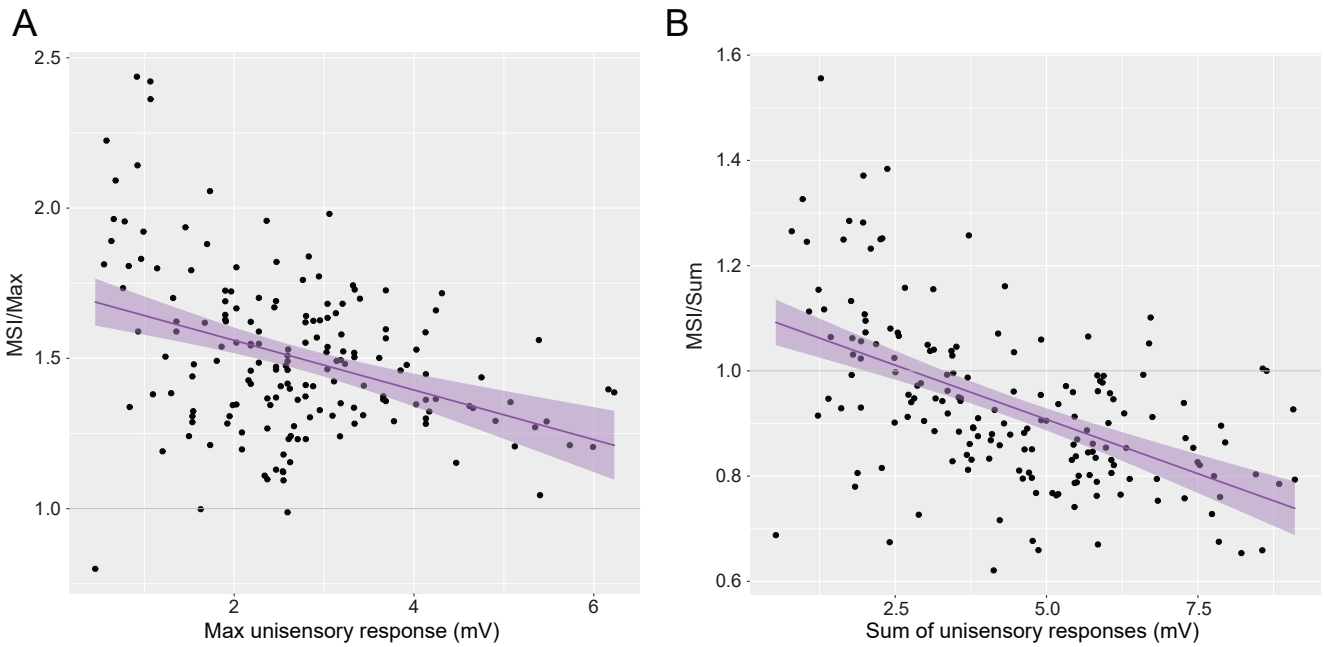

Figure 5. Multisensory integration of subthreshold unisensory stimuli. A. MSI/Max vs. the maximum unisensory response of different multisensory stimuli, irrespective of duration, frequency, or sequence of stimulation. B. Similar to A, but with the MSI/Sum instead vs. the sum of the unisensory responses.

Supplementary Figure 1

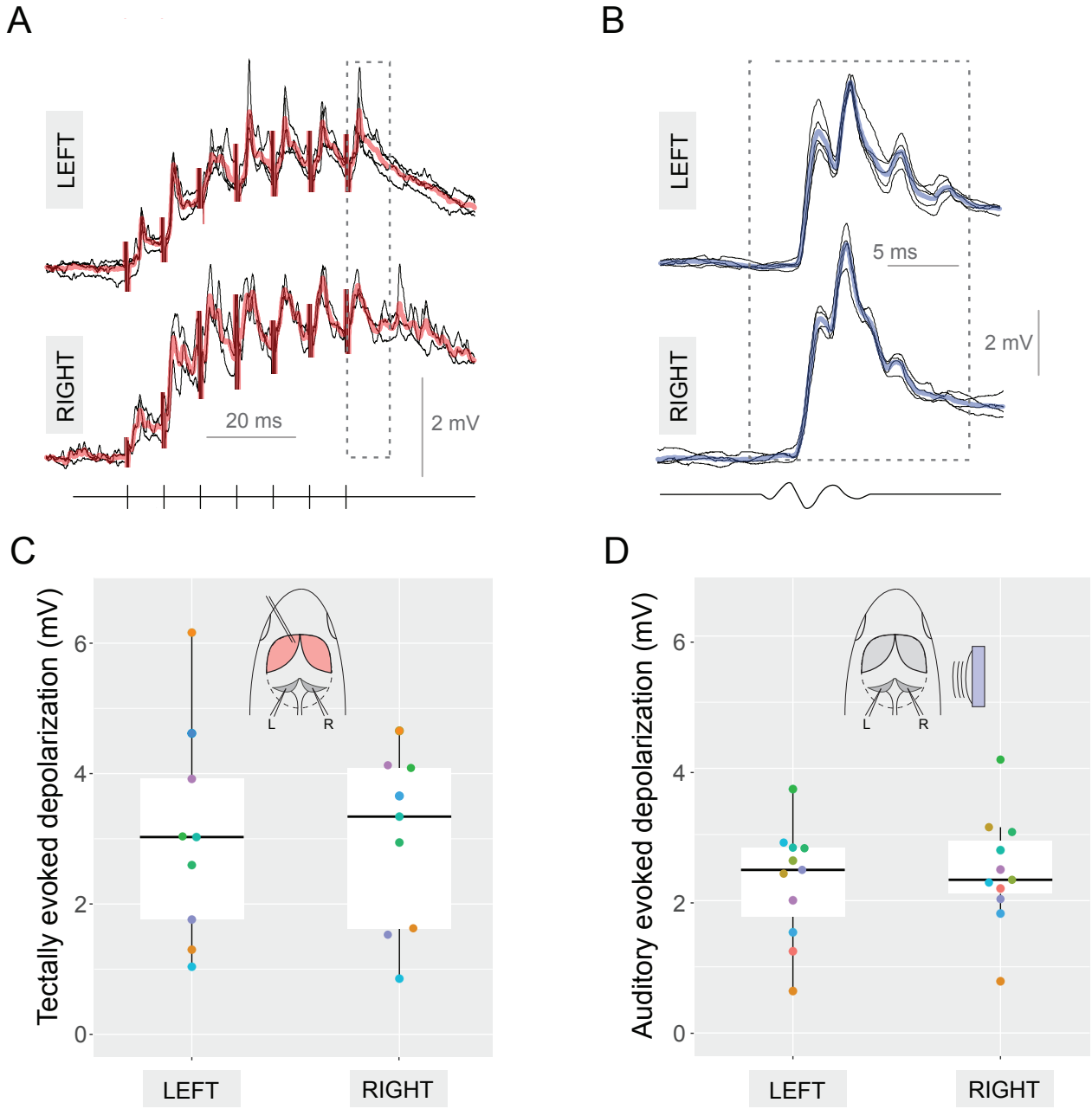

Supplementary Figure 1. A-B. Representative recordings of left or right M-cell somatic responses to an electric stimulus train delivered to the left tectum (A) or to a short 200 Hz sound pip produced by a loudspeaker placed to the right side of the fish (B). The mean (of 3-5 repetitions) response is shown in solid color and the diagram of the tectal stimulus or the sound pip are shown below the traces. Dashed boxes indicate the 12-ms time windows following the stimulus where the responses were quantified. C-D. Boxplots showing the median, upper and lower quartiles and comparing the response to the same stimulus in the left or right M-cell in 9 fish for the tectal stimulus (C) and 11 fish for the auditory stimulus (D). Markers with the same color in left and right belong to pairs of M-cells of the same fish. No differences were found in the evoked response amplitude between the left and right M-cells or for tectal or auditory stimuli.